Title	Structure of 136Sn and the Z = 50 magicity
Author(s)	Wang, He; Aoi, Nori; Takeuchi, Satoshi; Matsushita, Masafumi; Doornenbal, Pieter C.; Motobayashi, Tohru; Steppenbeck, David; Yoneda, Kenichiro; Baba, Hidetada; Dombrádi, Zs S.; Kobayashi, Kota; Kondo, Yosuke; Lee, Jenny; Liu, Hongna; Minakata, Ryogo; Nishimura, Dai; Otsu, Hideaki; Sakuraï, Hiroyoshi; Sohler, Dora; Sun, Yelei; Tian, Zhengyang; Tanaka, Ryuki; Vajta, Zs; Yang, Zaihong; Yamamoto, Tetsuya; Ye, Yanlin; Yokoyama, Rin
Citation	Progress of Theoretical and Experimental Physics, 2014, v. 2014, n. 2
Issued Date	2014
URL	http://hdl.handle.net/10722/200148
Rights	This work is licensed under a Creative Commons Attribution-NonCommercial-NoDerivatives 4.0 International License.

PTEP

Prog. Theor. Exp. Phys. **2014**, 023D02 (7 pages)
DOI: 10.1093/ptep/ptu003

Structure of ^{136}Sn and the $Z = 50$ magicity

He Wang[1,2,*], Nori Aoi[3], Satoshi Takeuchi[2], Masafumi Matsushita[4], Pieter Doornenbal[2], Tohru Motobayashi[2], David Steppenbeck[4], Kenichiro Yoneda[2], Hidetada Baba[2], Zsolt Dombrádi[5], Kota Kobayashi[6], Yosuke Kondo[7], Jenny Lee[2], Hong-Na Liu[1,2], Ryogo Minakata[7], Daiki Nishimura[8], Hideaki Otsu[2], Hiroyoshi Sakurai[2], Dora Sohler[5], Ye-Lei Sun[1], Zheng-Yang Tian[1], Ryuki Tanaka[7], Zsolt Vajta[5], Zai-Hong Yang[1], Tetsuya Yamamoto[3], Yan-Lin Ye[1], and Rin Yokoyama[4]

[1]*School of Physics and State Key Laboratory of Nuclear Physics and Technology, Peking University, Beijing 100871, China*
[2]*RIKEN Nishina Center, 2-1 Hirosawa, Wako, Saitama 351-0198, Japan*
[3]*Research Center for Nuclear Physics, Osaka University, Ibaraki, Osaka 567-0047, Japan*
[4]*Center for Nuclear Study, University of Tokyo, RIKEN Campus, Wako, Saitama 351-0198, Japan*
[5]*Institute for Nuclear Research, H-4001 Debrecen, Pf. 51, Hungary*
[6]*Department of Physics, Rikkyo University, 3-34-1 Nishi-Ikebukuro, Toshima, Tokyo 172-8501, Japan*
[7]*Department of Physics, Tokyo Institute of Technology, 2-12-1 Ookayama, Meguro, Tokyo 152-8551, Japan*
[8]*Department of Physics, Tokyo University of Science, 2641 Yamazaki, Noda, Chiba 278-8510, Japan*
*E-mail: wanghe@ribf.riken.jp

Received November 21, 2013; Accepted December 27, 2013; Published February 1, 2014

The first 2^+ excited state in the neutron-rich tin isotope ^{136}Sn has been identified at 682(13) keV by measuring γ-rays in coincidence with the one proton removal channel from ^{137}Sb. This value is higher than those known for heavier even–even $N = 86$ isotones, indicating the $Z = 50$ shell closure. It compares well to the first 2^+ excited state of the lighter tin isotope ^{134}Sn, which may suggest that the seniority scheme also holds for ^{136}Sn. Our result confirms the trend of lower 2^+ excitation energies of even–even tin isotopes beyond $N = 82$ compared to the known values in between the two doubly magic nuclei ^{100}Sn and ^{132}Sn.

Subject Index D13, D27

1. Introduction

Nuclei with a few valence particles or holes outside a doubly magic nucleus play an essential role in the study of nuclear structure. In particular, the properties of nuclei in the vicinity of ^{100}Sn and ^{132}Sn ($Z = 50$, $N = 82$) have attracted many studies in the past, as these nuclei are doubly magic while lying far away from the line of β stability. In addition, the long range of the Sn isotopic chain enables benchmark studies for the change of nuclear properties with greatly varying numbers of neutrons. It thus provides an opportunity to explore possible modifications in the shell structure beyond the two doubly magic nuclei toward the proton and neutron drip-lines. However, at present experimental knowledge for the tin isotopes heavier than ^{132}Sn is very limited and only exists up to ^{100}Sn on the proton-rich side [1].

For the neutron-rich tin isotopes, spectroscopic information beyond the ^{132}Sn core has been obtained experimentally only up to $N = 84$ [2–4]. The low-lying excited states in ^{133}Sn yield direct information on the single-particle states outside the $N = 82$ shell closure [2]. For ^{134}Sn, the energy

of the first 2^+ excited state ($E_x(2_1^+)$) was found to be much lower than that for ^{130}Sn [3], while the reduced transition probabilities between the 2_1^+ state and the ground state ($B(E2)$) are similar for those two nuclei [4]. This is very different from the case of heavier isotopic chains, such as Xe, Ba, and Ce, where $B(E2)$ increases as $E_x(2_1^+)$ decreases [5]. It is therefore intriguing to extend the studies towards more neutron-rich Sn isotopes in order to investigate possible structure changes in this region.

The structural evolution in the Sn isotopes beyond $N = 82$ has been discussed theoretically with shell-model calculations employing different realistic effective interactions [6–9]. These shell-model calculations showed a very different trend in the energies of low-lying excited states as a function of the neutron number. Using effective nucleon–nucleon interactions, constant $E_x(2_1^+)$ values are predicted in Refs. [7,8], while Ref. [9] shows a decrease in the 2_1^+ excitation energy beyond $N = 82$ with an empirical interaction. Different $E_x(2_1^+)$ behaviors have also been suggested by mean-field approaches with different interactions [10–12]. Therefore, the $E_x(2_1^+)$ systematics are critical to understanding the structures in the Sn isotopes beyond $N = 82$. In the present work, we report on the first 2^+ state in ^{136}Sn, which is the first spectroscopic study for this isotope with four valence neutrons in addition to the ^{132}Sn core.

2. Experiment

The experiment was carried out at the RIKEN Radioactive Isotope Beam Factory [13,14] operated by the RIKEN Nishina Center and the Center for Nuclear Study, University of Tokyo. The secondary beams including ^{137}Sb were produced by an in-flight fission reaction of a ^{238}U primary beam at 345 MeV/nucleon incident on a tungsten target. Secondary cocktail beams were selected and purified in the first stage of the BigRIPS fragment separator [15] by employing a wedge-shaped aluminum energy degrader with thickness of 0.8 g cm^{-2} at the dispersive focus. For a further purification, another 0.4 g cm^{-2} thick aluminum energy degrader was used in the second stage. Particle identification of the fission products was made event-by-event via the $\Delta E - B\rho -$ TOF (time of flight) method as described in Ref. [16] using a similar setup.

The secondary beams impinged on a 1.1 g cm^{-2} thick ^{9}Be target to induce the secondary reactions. At the middle of the secondary target, the average energy of ^{137}Sb isotopes was around 240 MeV/nucleon. Reaction products were analyzed by the ZeroDegree spectrometer [15] and again identified using the $\Delta E - B\rho -$ TOF method as for BigRIPS. The energy loss (ΔE) was measured by an ionization chamber located at the final focus to deduce the atomic number Z in combination with the time of flight, which was determined by two plastic scintillators placed at the entrance and the final focus of the ZeroDegree spectrometer. A trajectory reconstruction was made to determine the magnetic rigidity ($B\rho$) by position and angle measurements at the dispersive focus. With $B\rho$ and TOF information, the mass-to-charge ratio A/Q was obtained. In addition, a $LaBr_3$(Ce) scintillation detector located downstream of the ionization chamber was used for a total kinetic energy (TKE) measurement. The mass number (A) was obtained from the TKE–TOF correlation. Resolutions in Z, A/Q, and A for the Sn isotopes were 0.47 (FWHM—full width at half maximum), 6.5×10^{-3} (FWHM), and 1.5 (FWHM), respectively.

Figure 1(a) shows a two-dimensional plot of Z versus A/Q for the fragments produced from the ^{137}Sb secondary beams on the reaction target. The ^{136}Sn ions in the fully stripped ($Q = Z$) charge state are contaminated by the ^{133}Sn^{49+} ions in the hydrogen-like ($Q = Z - 1$) charge state as these two nuclei have similar A/Q values. Figure 1(b) displays a two-dimensional plot of A versus A/Q

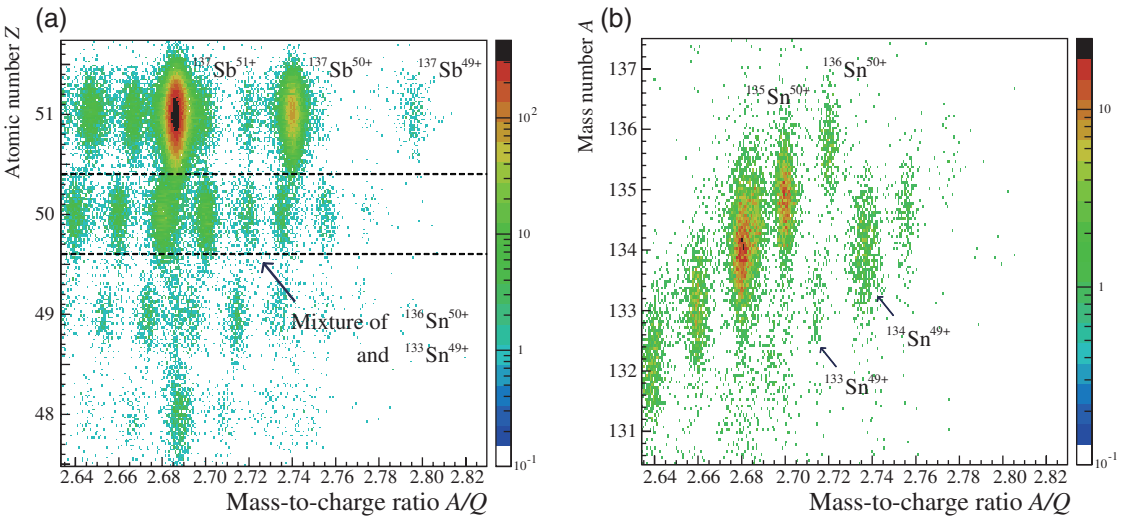

Fig. 1. Particle identification in the ZeroDegree spectrometer behind the reaction target. Panel (a) shows the two-dimensional plot of Z versus A/Q after selecting ^{137}Sb in the BigRIPS fragment separator. The horizontal dashed lines show the Z gate used to select the Sn isotopes. In Panel (b), the two-dimensional plot of A versus A/Q is displayed for the Sn isotopes. The fully stripped ^{136}Sn ions can be clearly separated from the ^{133}Sn^{49+} ions in the hydrogen-like charge state.

after selecting the Sn isotopes by the Z gate of $Z = 50.0 \pm 0.4$, as shown by the horizontal dashed lines in Fig. 1(a). The fully stripped ^{136}Sn fragments were unambiguously distinguished from the hydrogen-like ^{133}Sn^{49+} contaminants in the plot.

In order to detect the γ-rays emitted from decaying excited states, the secondary target was surrounded by the DALI2 spectrometer [17], which consisted of 186 NaI(Tl) scintillation detectors and covered the polar angles from 14 to 148 degrees with respect to the beam axis. The energy resolution and full energy peak efficiency were measured to be 9% (FWHM) and 22%, respectively, for the 0.662 MeV γ-rays emitted from a stationary ^{137}Cs source.

3. Results

The Doppler-shift-corrected γ-ray energy spectrum in coincidence with the ^{136}Sn isotopes produced via one proton knockout reactions from ^{137}Sb is shown in Fig. 2. A peak is clearly identified at 682(13) keV, which we attribute to the γ-ray decay from the 2_1^+ state to the ground state. The stated error of the energy includes statistical and systematic contributions. The latter is attributed to the uncertainties in the energy calibration (3 keV), and the ambiguities caused by the lifetime of the excited state as described in Ref. [18] causing an additional uncertainty of about 1% of the γ-ray energy. The experimental spectrum in Fig. 2 was fitted with a response function simulated with the GEANT4 [19] framework on top of an exponential background.

4. Discussion

In Fig. 3(a), the 2^+ excitation energies for the even–even $N = 86$ isotones are displayed as a function of the proton number. The first 2^+ excited state in ^{136}Sn is much higher than those for the neighboring nuclei, resulting in a concave pattern for the $E_x(2_1^+)$ systematics between $Z = 50$ and $Z = 62$. The high $E_x(2_1^+)$ value in ^{136}Sn indicates the presence of the $Z = 50$ magicity in the $N = 86$ isotones.

The isotopic dependence of $E_x(2_1^+)$ for the even–even Sn isotopes is shown in Fig. 3(b). The newly measured $E_x(2_1^+)$ value for ^{136}Sn is close to that for ^{134}Sn at 725 keV [3]. The constant $E_x(2_1^+)$ value

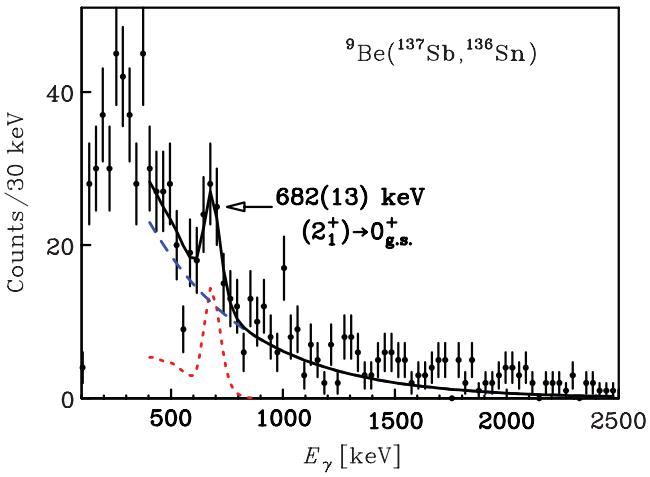

Fig. 2. Doppler-corrected γ-ray energy spectrum following the ^{9}Be(^{137}Sb, ^{136}Sn) reaction. The solid line shows a fit with a simulated response function at 682 keV (dotted line) on top of an exponential background (dashed line).

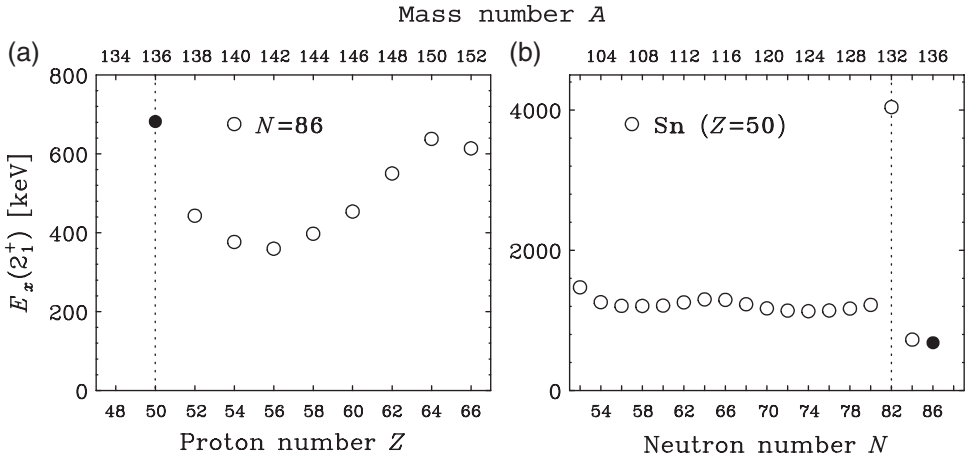

Fig. 3. Systematics of the 2_1^+ excitation energies. Panel (a) displays the experimental $E_x(2_1^+)$ (open circles) for the even–even $N = 86$ isotones as a function of the proton number. In Panel (b), the $E_x(2_1^+)$ values for the Sn isotopic chain are shown. The results of the present work are indicated by filled circles in both panels. Other values are taken from Ref. [5]. The error bars are smaller than the symbol sizes and the vertical dotted lines represent the magic numbers in both panels.

along the isotopic chain beyond ^{132}Sn at ^{134}Sn and ^{136}Sn is consistent with the characteristic of the seniority scheme. Indeed, in the lighter Sn isotopes the 2_1^+ excited state stays almost constant in a very wide region between the doubly magic nuclei of ^{100}Sn and ^{132}Sn, which can be understood by a dominance of the seniority $\nu = 2$ configuration [20,21], i.e., the excited states are created by breaking a neutron pair in the valence space. Our experimental finding of the similar $E_x(2_1^+)$ values for ^{134}Sn and ^{136}Sn may suggest that the seniority scheme also holds for the tin isotopic chain beyond $N = 82$ up to $N = 86$.

Another interesting feature of the $E_x(2_1^+)$ systematics along the tin isotopes is its asymmetric behavior between the two regions, one below $N = 82$ and the other above $N = 82$. The 2^+ excitation energies in ^{134}Sn [3] and ^{136}Sn are about 500 keV lower than those values for the lighter isotopes

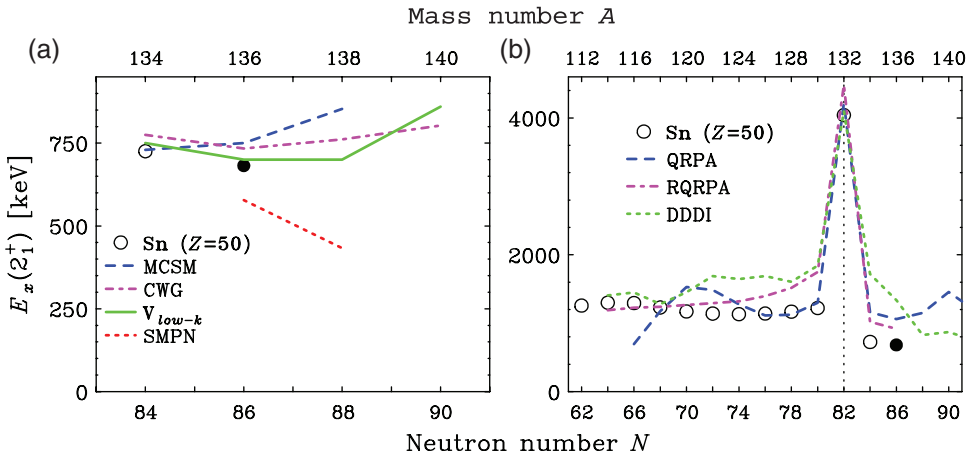

Fig. 4. The $E_x(2_1^+)$ systematics for the Sn isotopes beyond $N = 82$ (a), and with a wide range (b). The filled symbols are obtained in the present work and the open symbols are taken from Ref. [5]. In Panel (a), shell-model calculations with MCSM (dashed) [6], the CWG (dot-dashed) interaction [7], the V_{low-k} interaction (solid) [8], and the SMPN interaction (dotted) [9], are displayed for comparison. Panel (b) shows mean-field calculations using QRPA (dashed) [10], RQRPA (dot-dashed) [11], and the SHF method with paring forces DDDI (dotted) [12]. The vertical dotted line indicates the magic number $N = 82$. See text for details.

between $N = 50$ and $N = 82$ [5]. The $E_x(2_1^+)$ asymmetric pattern might be due to a reduction of the pairing energy in the $N > 82$ region, because $E_x(2_1^+)$ is determined mostly by the strength of the pairing under the seniority scheme. Indeed, a quenching in the pairing gap is suggested from the decrease of the odd–even staggering of masses in the Sn isotopes across $N = 82$ in the recent mass measurement [22]. Although several reasons were proposed, such as a low level density [22] or the large average distance between the valence nucleons [7], the origin of the weakening of the neutron pairing is not clear. It is interesting to note that the asymmetric $E_x(2_1^+)$ pattern seen in the Sn isotopes with respect to $N = 82$ is not seen in their valence mirror nuclei with proton number around $Z = 82$ in the $N = 126$ isotones, where the protons occupy the same orbitals as the neutrons in the vicinity of ^{132}Sn. This fact implies that the weakening of the neutron pairing is caused by the structure change characteristic in this neutron-rich Sn region beyond $N = 82$.

The 2_1^+ excited states in the Sn isotopes beyond $N = 82$ have been studied by several shell-model calculations [6–9]. All these calculations, as shown in Fig. 4(a), use the neutron $2f_{7/2}$, $3p_{3/2}$, $1h_{9/2}$, $3p_{1/2}$, $2f_{5/2}$, $1i_{13/2}$ single-particle orbitals between $N = 82$ and $N = 126$ and an inert ^{132}Sn core. Using the Hamiltonian obtained by reproducing the level scheme in ^{134}Sn [6], MCSM predicts a similar $E_x(2_1^+)$ value at ^{136}Sn to the one at ^{134}Sn and a slight increase in the 2_1^+ excitation energies for larger N. Calculations using different effective nucleon–nucleon interactions, denoted as CWG and V_{low-k}, respectively, show a nearly constant $E_x(2_1^+)$. The CWG [7] and V_{low-k} [8] interactions are derived from the CD-Bonn potential using the G matrix and constructing a low-momentum potential, respectively. The CWG calculations predict the dominance of the seniority $\nu = 2$ configuration in these excited states [7]. By using an empirical interaction, the SMPN [9] calculations show a smaller $E_x(2_1^+)$ at $N = 86$ and a decreasing trend up to $N = 88$. Most calculations (except for SMPN) can describe the 2_1^+ excited states of ^{136}Sn within an accuracy of about 40 keV. However, the SMPN predicts the $E_x(2_1^+)$ value at ^{136}Sn about 110 keV lower than our experimental findings. The fair agreement between the shell-model calculations and our results indicates that ^{136}Sn can be basically described by the configurations with four valence neutrons outside the ^{132}Sn core.

The $E_x(2_1^+)$ values for a wide range of the Sn isotopic chain have also been calculated by mean-field approaches [10–12], as shown in Fig. 4(b). The dashed line represents the QRPA calculations with the Skyrme force SLy4 [10], while the dot-dashed line exhibits the relativistic QRPA (RQRPA) calculations using the NL3 effective interaction and Gogny's paring forces (D1S) [11]. Both of these calculations predict similar $E_x(2_1^+)$ values for $N = 84$ and $N = 86$. The Skyrme–Hartree–Fock (SHF) model using a short-range paring force, namely, the density-dependent δ interaction (DDDI) [12], exhibits a steep decrease up to ^{138}Sn beyond $N = 82$. The RQRPA calculation shows an asymmetric pattern around $N = 82$; however, it overestimates the $E_x(2_1^+)$ values toward $N = 82$. The asymmetry is not reproduced by the QRPA and SHF calculations, although QRPA shows a good agreement with the lighter Sn isotopes. It seems that the two features, namely the constant $E_x(2^+)$ values beyond $N = 82$ and the asymmetry around $N = 82$ as mentioned above, cannot be reproduced at the same time by these calculations.

5. Summary

In summary, the first 2^+ excited state in ^{136}Sn has been identified for the first time by measuring γ-rays in conjunction with the one proton removal channel from ^{137}Sb. The measured $E_x(2_1^+)$ value of 682(13) keV in ^{136}Sn was found to be much higher than the neighboring $N = 86$ isotones, indicating a good $Z = 50$ shell closure. The $E_x(2_1^+)$ value stays almost constant in ^{134}Sn and ^{136}Sn, which suggests that the seniority scheme holds beyond $N = 82$ up to $N = 86$. The asymmetric pattern in the $E_x(2_1^+)$ systematics in the Sn isotopes above and below $N = 82$ might be due to the reduction of the pairing energy. Our result is fairly well produced by shell-model calculations while the mean-field approaches cannot reproduce the constancy of $E_x(2_1^+)$ and the asymmetry in the Sn isotopic chain at the same time. Further studies on the evolution of the 2_1^+ excitation energies in more neutron-rich tin isotopes with $N > 86$ are encouraged to see if the constancy in the 2_1^+ and higher excited states persists.

Acknowledgments

We acknowledge the RIKEN Nishina Center accelerator staff for providing the ^{238}U primary beam and BigRIPS team for their effort on tuning the secondary beam. The authors Z.D., D.So., and Z.V. were supported by OTKA Grants No. K100835 and NN104543.

References

[1] C. B. Hinke et al., Nature **486**, 341 (2012).
[2] K. L. Jones et al., Nature **465**, 454 (2010).
[3] A. Korgul et al., Eur. Phys. J. A **7**, 167 (2000).
[4] D. C. Radford et al., Nucl. Phys. A **746**, 83 (2004).
[5] NNDC. *National Nuclear Data Center*. (Brookhaven National Laboratory, Upton, NY, 2013). (Available at: http://www.nndc.bnl.gov/, date last accessed 11 January 2014).
[6] N. Shimizu, T. Otsuka, T. Mizusaki, and M. Honma, Phys. Rev. C **70**, 054313 (2004).
[7] M. P. Kartamyshev, T. Engeland, M. Hjorth-Jensen, and E. Osnes, Phys. Rev. C **76**, 024313 (2007).
[8] A. Covello, L. Coraggio, A. Gargano, and N. Itaco, J. Phys. Conf. Ser. **267**, 012019 (2011).
[9] S. Sarkar and M. Saha Sarkar, Phys. Rev. C **81**, 064328 (2010).
[10] J. Terasaki and J. Engel, Phys. Rev. C **74**, 044301 (2006).
[11] A. Ansari, Phys. Lett. B **623**, 37 (2005).
[12] P. Fleischer, P. Klüpfel, and P.-G. Reinhard, Phys. Rev. C **70**, 054321 (2004).
[13] Y. Yano, Nucl. Instrum. Meth. B **261**, 1009 (2007).
[14] H. Okuno, N. Fukunishi, and O. Kamigaito, Prog. Theor. Exp. Phys. **2012**, 03C002 (2012).

[15] T. Kubo et al., Prog. Theor. Exp. Phys. **2012**, 03C003 (2012).
[16] T. Ohnishi et al., J. Phys. Soc. Jpn. **79**, 073201 (2010).
[17] S. Takeuchi, T. Motobayashi, H. Murakami, K. Demichi, and H. Hasegawa, RIKEN Accel. Prog. Rep. **36**, 148 (2003).
[18] P. Doornenbal et al., Phys. Rev. Lett. **103**, 032501 (2009).
[19] S. Agostinelli et al., Nucl. Instrum. Meth. A **506**, 250 (2003).
[20] R. F. Casten and B. M. Sherrill, Prog. Part. Nucl. Phys. **45**, S171 (2000).
[21] I. Talmi. *Simple Models of Complex Nuclei* (Harwood Academic Publisher, New York, 1993).
[22] J. Hakala et al., Phys. Rev. Lett. **109**, 032501 (2012).